Thermochemical energy storage performance of copper oxides: Effect of support materials

Journal of Energy Storage 32 (2020) 102012

Contents lists available at ScienceDirect

Journal of Energy Storage

journal homepage: www.elsevier.com/locate/est

Thermochemical energy storage performance of copper oxides: Effect of support materials

Duygu Yilmaz *, Esraa Darwish, Henrik Leion

Chalmers University of Technology, Chemistry and Chemical Engineering, 412 58, Gothenburg, Sweden

ARTICLE INFO

Keywords:
Thermochemical energy storage
Copper oxides
Oxygen carriers

SUMMARY

Thermochemical energy storage (TCES) is one of the most promising methods for utilization of solar energy. Metal oxides can exhibit reversible redox reactions that are useful for TCES applications. Especially, transitional metal oxides can undergo reduction reactions at high temperatures while absorbing energy given to the system. Later on, when the temperature goes down below a phase-transition temperature, exothermic re-oxidation reactions can take place. Air can be used both as oxygen source and heat transfer medium during the redox reactions. Recently, several studies have been published about the utilization of metal oxides for TCES applications. Among these metal oxides, copper oxides received a great attention owing to its cyclic stability and suitable redox temperature. In this study, copper oxides are used as energy storage material in combination with ZrO_2, ZrO_2-La_2O_3, $MgAl_2O_4$, $Mg_2Al_2O_4$-La_2O_3, CeO_2, CeO_2-La_2O_3 as support materials. The best results were obtained from samples supported with $MgAl_2O_4$, $Mg_2Al_2O_4$-La_2O_3. This most likely eventuated due to the other reversible phase transformations that take place in these systems such as formation of $LaAlO_3$ and $Cu_2Al_2O_4$. Especially $Mg_2Al_2O_4$-La_2O_3 addition improved the system, both in terms of cyclic stability and heat capacity.

1. Introduction

Thermochemical energy storage (TCES) is a very promising technology which enables to address intermittent problems in renewable energy technologies, especially solar energy [1–5]. Continuous electricity production becomes possible with storing the energy during on-sun hours and releasing the stored energy during off-sun hours [6].

TCES exhibits better performance regarding to energy storage density (0.5-1 kWh/kg) [7], and storage within a large temperature range (25-1000°C) [8] among the other thermal energy storage techniques such as latent and sensible heat storage. In addition to this, there is no need to use complex storage procedures as the heat is stored in the form of chemical energy in TCES [9]. To store high amount of energy, redox reactions of metal oxides can be useful since their operational temperatures are relatively high [10]. For TCES applications, properties of the storage materials such as cyclic stability and agglomeration tendency are crucially [7,11,12].

From metal oxides, Co_3O_4, CuO and Mn_2O_3 exhibit sufficient performance to meet the expectations for TCES applications [13–15]. Among these oxides, Cu based oxides are also outstanding as they exhibit high energy storage capacity (811 kJ/kg for CuO) and oxygen uncoupling ability [16,17]. From this point of view, CuO becomes very suitable as its usage would access more flexible design and process parameters for TCES applications [18,19]. The general reaction scheme for Cu oxides is given below (1).

$$4\ CuO(s) + \Delta H_r \leftrightarrow 2Cu_2O(s) + O_2(g) \quad (1)$$

However, occurrence of sintering due to both highly exothermic reaction nature of discharging step and comparably low Hüttig and Tammann temperatures of the copper oxide may cause the loss of cyclic stability and reactivity [8,20]. Hüttig and Tammann temperatures define as $0.3T_m$ and $0.5T_m$ (Tm is the melting point of the material) of the materials respectively and these temperatures indicate the onset of sintering temperature [21].

In the literature, high degree of reduction and high temperatures have been reported as conditions which should be avoided in case of CuO being used [22,23]. To overcome this problem, support materials have been commonly reported in similar applications in which cyclic stability and reactivity are important parameters [24,25]. Therefore, CuO could be supported by other oxide materials to increase the operational temperature of the application. Support materials are mainly used to decrease the sintering effect and supply additional vacant or

* Corresponding author.
E-mail address: duyguy@chalmers.se (D. Yilmaz).

https://doi.org/10.1016/j.est.2020.102012
Received 27 May 2020; Received in revised form 14 September 2020; Accepted 14 October 2020
Available online 28 October 2020

available sites for oxygen and catalyst surface during redox reactions [26,27]. In the literature about redox of Cu based oxides there are plenty of support materials such as Al_2O_3, ZrO_2, SiO_2, TiO_2, $MgAl_2O_4$ and CeO_2 [21,22,28]. Among these support materials, $MgAl_2O_4$ was reported to provide sufficient physical stability and reactivity and ZrO_2 was reported as to decrease defluidization and agglomeration tendency [25,29]. CeO_2 was also used as a support material with CuO resulting in high reactivity [30]. In addition, using La_2O_3 in CuO-ZrO_2 and CuO-$MgAl_2O_4$ increased the oxygen releasing ability and the agglomeration resistance [31,32].

In this study CuO with ZrO_2, ZrO_2-La_2O_3, $MgAl_2O_4$, $MgAl_2O_4$-La_2O_3, CeO_2 and CeO_2-La_2O_3 as support materials were used to investigate their thermochemical energy storage performance. Samples were tested in a fluidized bed reactor with a cyclic heating and cooling procedure. Simultaneous thermal analysis was also carried out to investigate the thermal characteristics of the samples. Phase analysis were carried out by X-Ray Diffraction to reveal the present phases both before and after the tests. Reaction mechanisms were also supported by thermodynamic equilibrium calculations.

2. Experimental procedure

The samples consisting of CuO (Trimanox®, Chemalloy™), ZrO_2 (Silverbond M800®, Sibelco™), La_2O_3, $MgAl_2O_4$ and CeO_2 used in this study were produced by VITO^{TM} using spray-drying. Raw materials with different composition (Table 1), organic binders and dispersants were dispersed in deionized water and mixed homogeneously. The water based suspension was then pumped into a hot drying chamber to obtain small solid loaded droplets. The spray-dried particles were sieved into 125-180 μm followed by calcination at 1100°C for 4 h in air. Table 1 also present works where these materials have been used before as oxygen carriers in chemical looping oxygen uncoupling (CLOU) applications.

Phase analysis of the samples both before and after being used in the cyclic experiments were done with XRD (Bruker^{TM} D8 Advance, Cu-Kα, 40 kV, 40 mA) in the 2-theta range of 15-80° with a step size of 0.01. Scanning electron microscopy (SEM-Zeiss LEO Ultra 55 FEG) was used to investigate the morphological characteristics. For secondary electron imaging 10.0 kV acceleration voltage and 10.0 mm working distance were used. To verify the experimentally observed interaction, thermodynamic equilibrium calculations were carried out using FactSage 7.2 software with the FactSage-Equilibrium Module, under the presumption of an isothermal and standard state with the use of Pure Substance (FactPS)-Oxide (FToxid) databases. The equilibrium calculations were based on the Gibbs energy minimization method.

For thermal analysis, simultaneous thermal analyzer (Netzsch™-STA 409 PC Luxx) was used to determine the thermal characteristics of the samples with changing the temperature between 600-1000°C as cycles. During the experiments, STA was flushed by air flow and N_2 as purge gas.

To investigate the redox and oxygen release characteristics of the samples, several heating and cooling steps were implemented in a fluidized bed reactor that has a length of 820 mm and a porous quartz plate of 22 mm in diameter placed 370 mm from the bottom [38]. The scheme of the fluidized bed setup is given in Figure S1 (Supplementary Material). For each experiment, the amount of sample was 10 g. The reduction and oxidation cycles were initiated by changing the temperature between 600°C and 1000°C for each cycle. It was reported that fixed partial pressure of O_2, especially lower than 0.05 atm, results in different degree of oxygen deficiency in an O_2 release capable compound [21,39]. For this reason, the system was flushed by a gas mixture consisting of 5 vol.% O_2 (0.05 atm) which was obtained by N_2 diluted in air during all cycles. In one of the experiments, air was directly used without dilution of N_2 to investigate the effect of O_2 partial pressure on the system. The O_2 level in the gas were detected by a Rosemount™ NGA 2000 multicomponent gas analyzer.

Table 1
Chemical composition of the copper oxide based powders used in this study and the reference works used the same materials in the literature.

Sample Name	Chemical Composition (wt.)	Ref.
CZ	40% CuO, 60% ZrO_2	[22,26,29,33,34]
CZL	40% CuO, 55% ZrO_2, 5% La_2O_3	[22,31]
CM	40% CuO, 60% $MgAl_2O_4$	[22,25,34–36]
CML	40% CuO, 55% $MgAl_2O_4$, 5% La_2O_3	[22,37]
CC	40% CuO, 60% CeO_2	[22,30]
CCL	40% CuO, 55% CeO_2, 5% La_2O_3	[22,31]

3. Results

As fluidized bed reactors have been reported as promising for thermochemical energy storage applications [18,40,41], investigation of the cyclic stability and oxygen releasing ability of the samples have in this work been carried in the fluidized bed. In the cyclic stability tests, the material was placed into the fluidized bed and cyclically heated up to 1000°C and cooled down to 600°C. Each cycle took on average 20 minutes. The temperature of the bed was measured by a thermocouple which was placed in the middle of the bed in the hot zone of the quartz reactor. When the temperature reached ~1000°C in the bed, the set point was decreased to 600°C, manually. In the cyclic stability test figures, the peaks shown on the upper part (yellow) represent the temperature changes in the bed. The peaks shown on the bottom part (blue) represent the observed O_2 concentration level in the gas analyzer connected to the reactor. The quantity of O_2 released/captured during the redox reactions is related to the reaction extent that corresponds to the amount of stored/released energy by the material [41,42]. In addition to this, the same amount of O_2 release and consumption in each cycle during the multi-cycle redox processes is consider as a sign of good cyclic stability [42–46].

Fig. 1 shows the cyclic stability test of the ZrO_2 supported CuO sample in the fluidized bed. In all experiments, the first cycle was excluded, since the first cycle is affected by the instrumental issues such as drift or temperature changes and is also influenced by how the sample was stored and treated before the experiments. Both for oxidation and reduction, very stable peaks were observed during the test. It has been reported that pure copper oxides exhibit strong agglomeration as the melting point of the material is close to the process temperature range [19]. Agglomeration is one of the main reasons for decreased redox activity of the materials [47]. From this point of view, ZrO_2 as support material for cyclic stability of CuO performed very well. During the cyclic stability test, re-oxidation peak point was observed at 900°C reaching min. peak point of 1,8vol.%O_2 in the outgoing gas while reduction was occurred at 1020°C reaching max. peak point of 10,99vol.% O_2. The average mass change was observed via STA (simultaneous thermal analysis) for the same CZ sample with 0,8 wt.% and 1 wt.% during oxidation and reduction, respectively. In STA, the cycles were also stable, and the average re-oxidation and reduction peak temperatures were observed as 920 and 990°C, respectively. In addition to this, the peak areas which indicate the relative reaction enthalpies for oxidation and reduction were studied by using Netzsch Proteus^{TM} Software(Figure S2). Using the energy calibration, the specific energy content was calculated as 440 and 305 kJ/kg CZ for reduction and oxidation, respectively. XRD analysis on CZ samples, both fresh and after being tested in fluidized bed, revealed that there is no observed chemical interaction between CuO/Cu_2O and ZrO_2. This was also verified by thermodynamic equilibrium calculations (TEC).

As mentioned in the introduction, La_2O_3 has been reported as a promising support material for increasing the agglomeration resistance of CuO [22,32]. For this reason, La_2O_3 was used as a support material for CuO together with ZrO_2(CZL). The cyclic stability of the material in the fluidized bed is shown in Fig. 2. The CZL sample, similar to CZ, also showed stable cyclic behaviour with a higher amount of average oxygen release starting at 1025°C (max. peak point of 12,11vol.%O_2) and

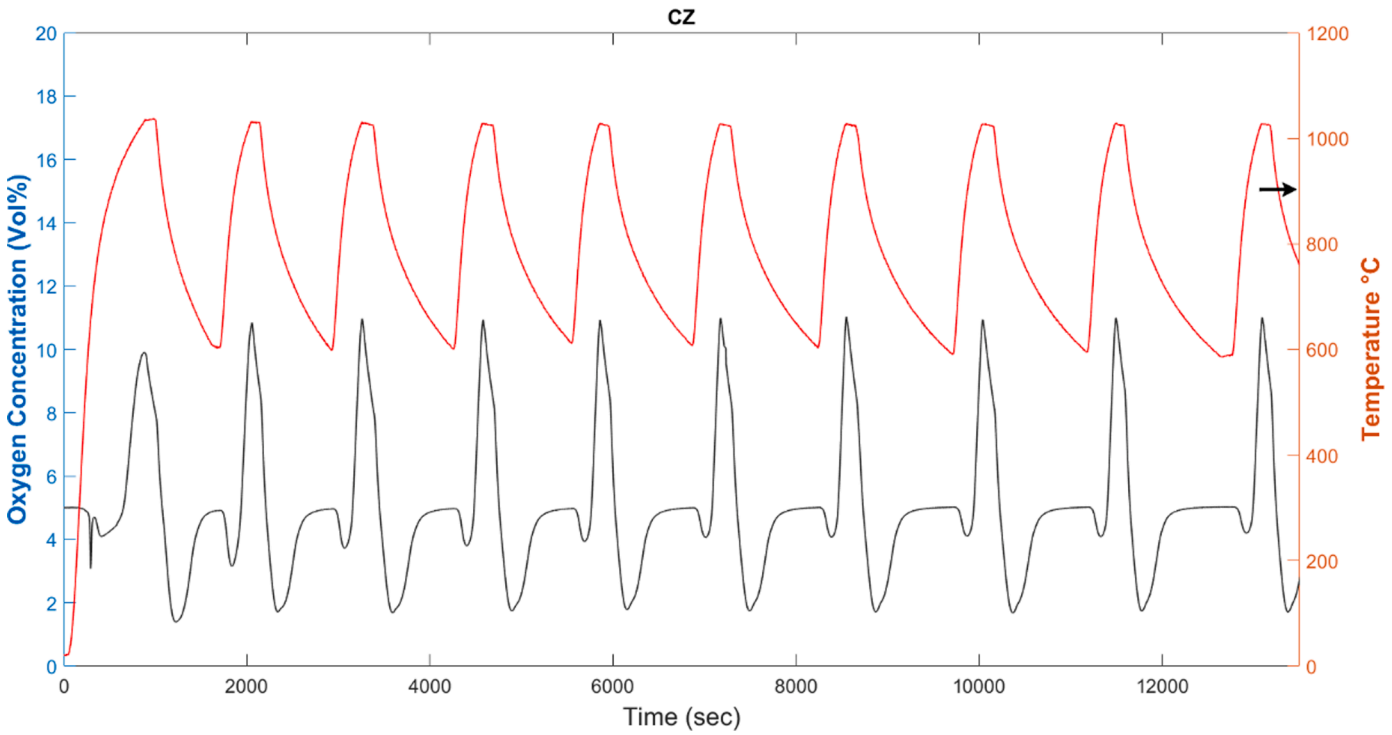

Fig. 1. Cyclic stability of the ZrO_2 supported CuO sample in the fluidized bed test.

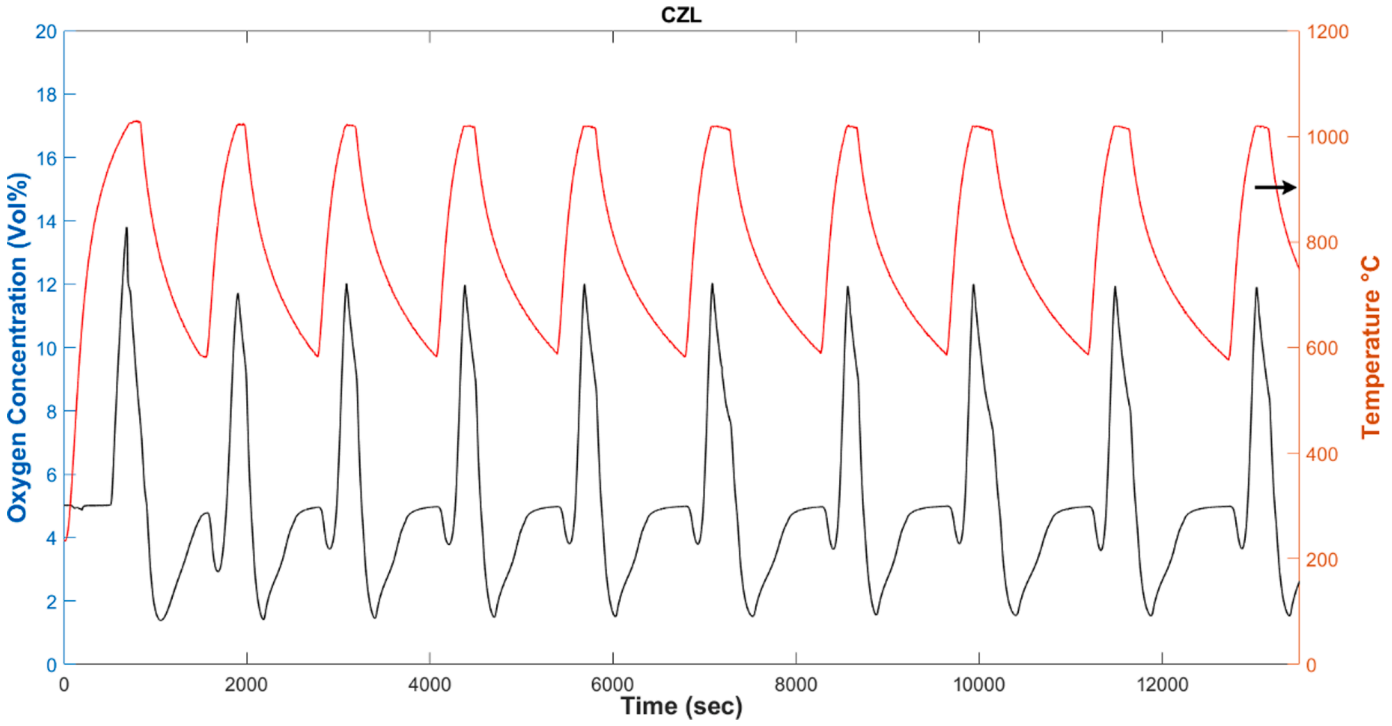

Fig. 2. Cyclic stability of the ZrO_2-La_2O_3 supported CuO sample in the fluidized bed test.

consumption starting at 890°C (min. peak point of 1,46vol.%O_2). The thermal behaviour of the sample was also stable in STA and the average re-oxidation peak temperature was observed as 920°C, similar to CZ while the average reduction temperature was a little bit lower than CZ at 980°C. The average weight loss was 1,3wt.% during reduction and the average weight gain was 1 wt.% during oxidation. The specific energy content of the sample was calculated as 250 and 230 kJ/kg CZL for reduction and oxidation, respectively. Similar to CZ, thermodynamic equilibrium calculations and XRD analysis after experiments also revealed that starting phases could form no new compounds during cycles.

When $MgAl_2O_4$ (CM) was used as a support material for CuO, the O_2 release performance was significantly better than CZ and CZL. The stability of the sample was outstanding both for reduction and oxidation

(Fig. 3). The average reduction peak temperature was 1010°C with the maximum 16,51 vol.%O_2 concentration while the average re-oxidation peak temperature was 870°C with the minimum 0,53 vol.% O_2 concentration in the fluidized bed tests. The cycle was also stable in STA and the average weight loss and weight gain were 1,01 and 1,06wt.%, respectively. The observed reduction peak temperature was 985°C which was similar to CZ and CZL. However, the observed average oxidation peak temperature was 930°C which is slightly higher than CZ and CZL. The specific energy content of the sample was calculated as 640 and 425 kJ/kg CM for reduction and oxidation, respectively. Thermodynamic equilibrium calculations suggested that there is a possible endothermic reaction (2) during reduction which may increase the agglomeration resistance of copper oxides as the reaction is reversible and the $Cu_2Al_2O_4$ has a higher melting point than pure Cu_2O [48]. Since this reaction is not thermodynamically favourable below 900°C, there was no observed phases in XRD related to this. However, oxidation of $Cu_2Al_2O_4$ into CuO and reforming of $MgAl_2O_4$ spinel is thermodynamically favourable during oxidation. From this point of view, $MgAl_2O_4$ is a promising candidate as support for CuO for TCES applications.

$$Cu_2O + MgAl_2O_4 \rightarrow Cu_2Al_2O_4 + MgO \quad (2)$$

When La_2O_3 was also used as a support material together with $MgAl_2O_4$ spinel (CML sample), the results were even more promising. Fig. 4 shows the cyclic stability of CML in the fluidized bed test. CML performed outstanding cyclic stability with the highest O_2 release/consumption among the samples we tested in this study. For CML, the minimum and maximum O_2 concentration during oxidation and reduction were observed as 0,54 vol.% O_2 and 16,71 vol.%O_2, respectively. The average peak temperature was 820°C and 1010°C for re-oxidation and reduction, respectively. Thermal gravimetric behaviour of the material was also stable in STA analysis. Similar to the samples tested, the average peak temperature was 920°C for oxidation and 970°C for reduction which is slightly lower than others. However, the average weight loss was observed as 3,07 wt.% during reduction which is significantly higher than samples tested in this study. Similar to this, the average weight gain was obtained as 1,24 wt.%. As already mentioned above, the weight changes during redox is related to the energy storage capacity of the system. From this point of view, CML exhibited the best performance among the tested samples as it showed the highest weight gain and weight loss in STA analysis. The specific energy content of the sample was calculated as 925 and 1050 kJ/kg CML for reduction and oxidation, respectively. However, the obtained weight changes during redox reactions were still lower than maximum theoretical weight changes for a CuO/Cu_2O redox systems with 60% support. This deviation may be caused by the effect of heating/cooling rates, particle size and distrubition of the samples and the amount of used mass as it is known that thermodynamic and kinetic factors are limiting the redox reactions [16,26,49,50].

In Fig. 5, cyclic stability of CC (CeO_2 supported CuO) was shown. Among the tested samples, CC showed the poorest O_2 release/consumption capacity, even though the redox cycles were very stable. During the fluidized bed test, generally reduction reaction reached the peak point at 1020°C, while this was 840°C for re-oxidation. On average, the maximum obtained O_2 concentration was 11,2 vol.%O_2 during reduction and minimum obtained O_2 concentration was 1,76 vol.%O_2 during oxidation which is similar to other samples. However, the cyclic stability was not stable as the others in thermal analysis. For STA, the reduction took place at maximum 990°C with the average weight loss around 0,5 wt%. In addition to this, re-oxidation in STA took place at maximum 950°C with the weight gain around 0,5 wt%. La_2O_3 addition to CeO_2 as support material for CuO (CCL), increased the O_2 release/consumption ability compare to CC. However, the performance of CCL could not reach the performance of the other tested samples. A good thing about this sample was the almost perfect cyclic behaviour which is important for material`s lifetime [51]. For CCL(Fig. 6), re-oxidation generally started to occur at 820°C and average O_2 concentration obtained was 0,25 vol.% during oxidation. These values were 1020°C and 12,58 vol.%O_2 for reduction peak and the highest obtained O_2 concentration, respectively. The cyclic stability of CCL was significantly better than CC in STA. In STA, the sample lost weight around 0,8 wt.% during reduction which generally took place at 980°C as peak maximum. For re-oxidation, the temperature was 920°C and the average weight gain was 0,7 wt.%.

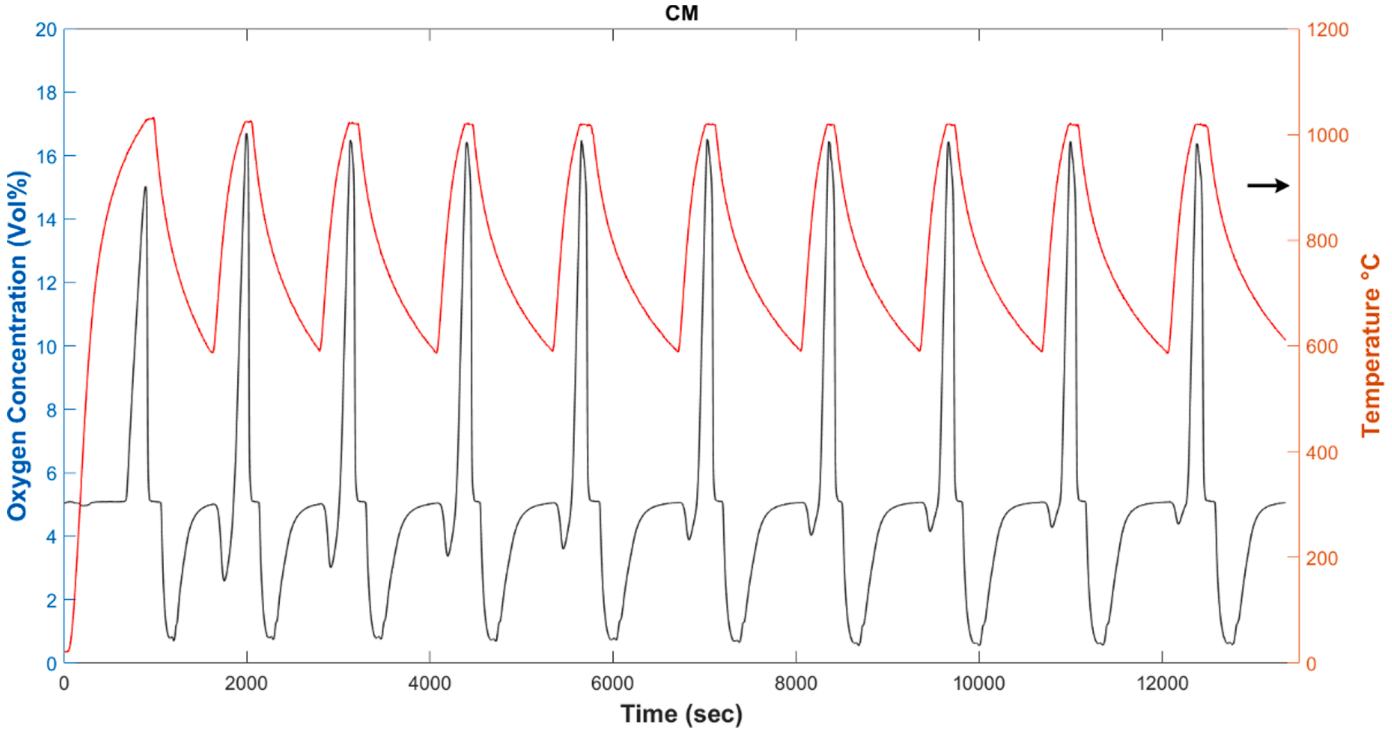

Fig. 3. Cyclic stability of the $MgAl_2O_4$ supported CuO sample in the fluidized bed test.

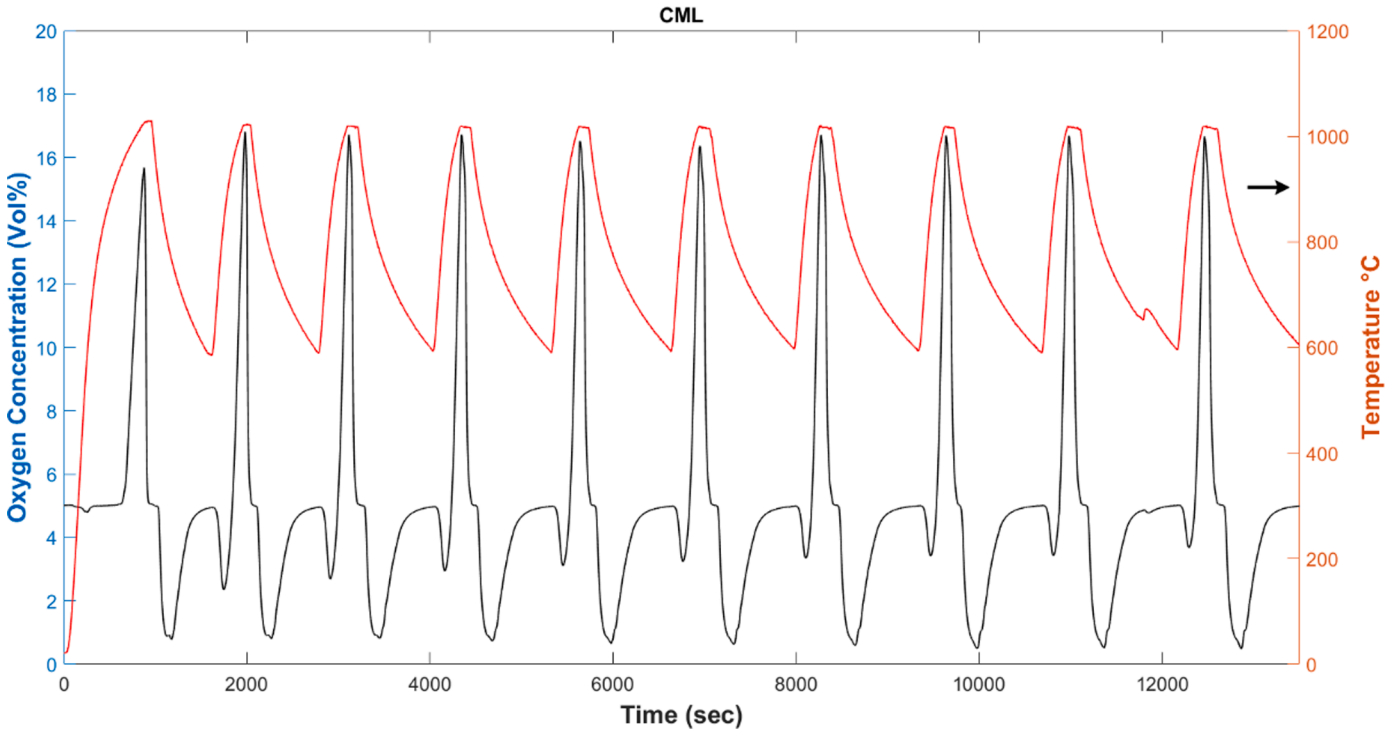

Fig. 4. Cyclic stability of the $MgAl_2O_2$-La_2O_3 supported CuO sample in the fluidized bed test.

A general overview of phase changes of the used materials can be seen in Table 2. This table includes both starting phases in the fresh samples and observed phases in the used samples after being tested in the fluidized bed is shown. Additionally, thermodynamic equilibrium calculations were also done to see how much the system differs from the thermodynamic equilibrium conditions. Formations of $La_2Zr_2O_7$, $LaAlO_3$ and $Ce_{0,75}La_{0,25}O_2$ were observed in the CZL, CML and CCL, respectively. To avoid the possible deactivation of active sites, support materials should not form any compound with CuO/Cu_2O. However, these compounds do not show any interaction towards CuO/Cu_2O. On the contrary, these formations may be the reason of the slight increase of the cyclic stability for CZ-CZL, CM-CML and CC-CCL. Especially $LaAlO_3$ is known a potential candidate for energy storage applications [52]. In addition to this, $LaAlO_3$ has a high melting point (2138°C) [53]. Therefore, it does not contribute to the agglomerate formation in the system. Overall, it is clear that CML has a great potential for this study.

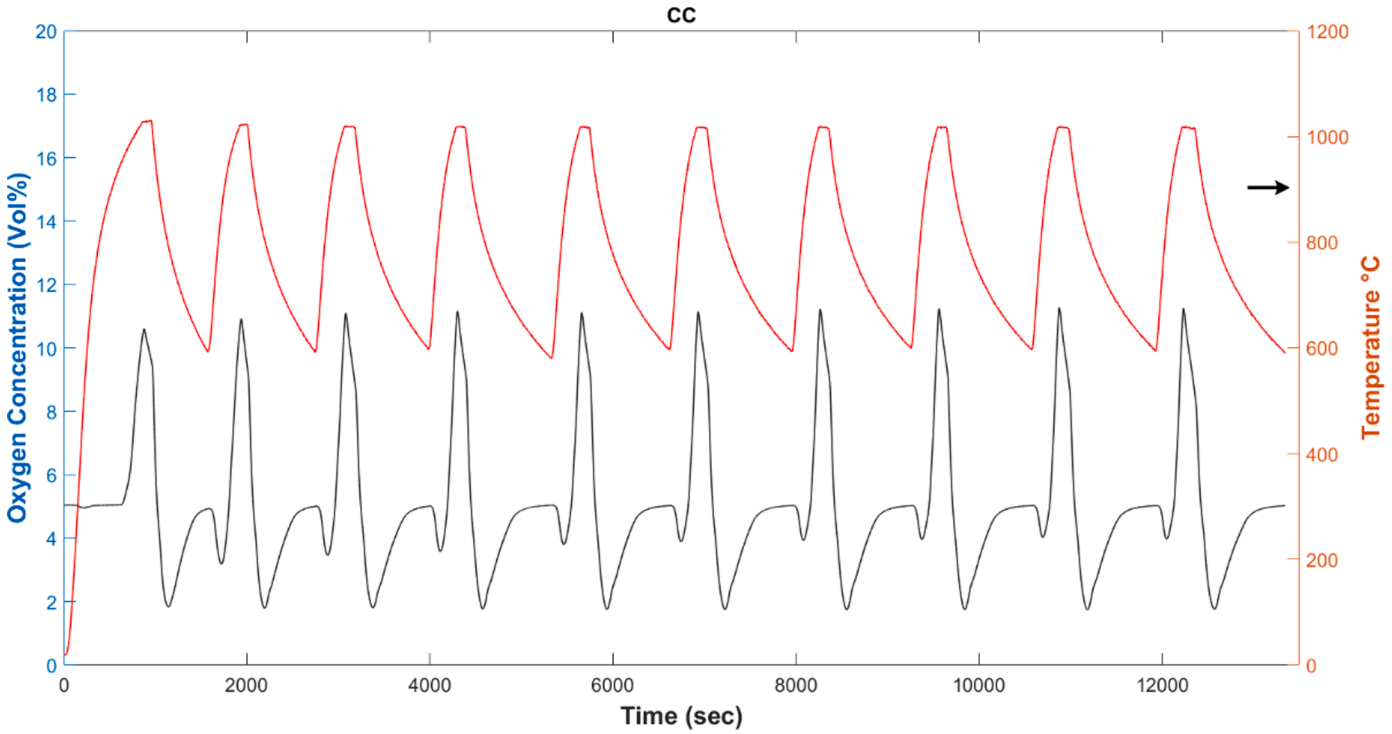

Fig. 5. Cyclic stability of the CeO_2 supported CuO sample in the fluidized bed test.

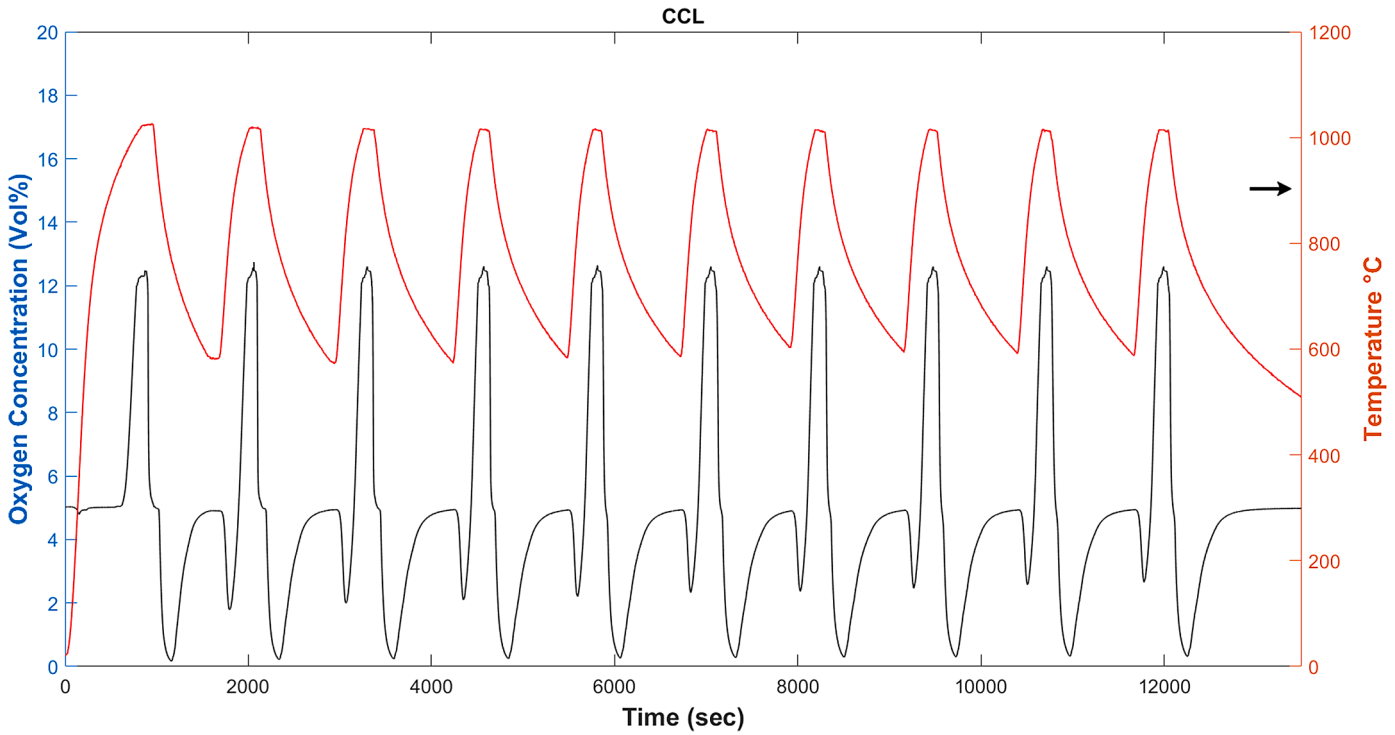

Fig. 6. Cyclic stability of the CeO_2-La_2O_3 supported CuO sample in the fluidized bed test.

Table 2
Phases revealed by XRD analysis in the starting samples and observed ones after the cyclic stability tests.

Sample	Starting Phases	Observed Phases After Tests	Calculated Phases by TEC
CZ	CuO, ZrO_2	CuO, ZrO_2	CuO, ZrO_2
CZL	CuO, ZrO_2, La_2O_3	CuO, ZrO_2, $La_2Zr_2O_7$	CuO, ZrO_2, La_2O_3
CM	CuO, $MgAl_2O_4$	CuO, $MgAl_2O_4$	CuO, $MgAl_2O_4$
CML	CuO, $MgAl_2O_4$, La_2O_3	CuO, $MgAl_2O_4$, $LaAlO_3$	CuO, MgO, $MgAl_2O_4$, $LaAlO_3$
CC	CuO, CeO_2	CuO, CeO_2	CuO, CeO_2
CCL	CuO, CeO_2, La_2O_3	CuO, CeO_2, La_2O_3, $Ce_{0,75}La_{0,25}O_2$	CuO, CeO_2, La_2O_3

To investigate further the best of the materials, CML, XRD analysis was carried out for fresh and tested sample (Fig. 7). Fresh CML, consisting of CuO (PDF Card No: 48-1548), $MgAl_2O_4$ (PDF: 04-007-2712) and La_2O_3 (PDF: 04-015-5007), formed some perovskite-type $LaAlO_3$ (PDF: 04-18-6998) during fluidized bed test. Formation of $LaAlO_3$, which most likely formed via Reaction 3, was also confirmed by thermodynamic equilibrium calculations.

$$MgAl_2O_4 + La_2O_3 \rightarrow MgO + 2\ LaAlO_3 \quad (3)$$

$LaAlO_3$ was reported as a good candidate for solar thermochemical applications due to its stability under redox conditions [52]. Most likely, together with $MgAl_2O_4$, it increased the physicochemical stability of the sample during redox reactions. To reveal the physicochemical condition of the particles, scanning electron microscope was used in secondary electron mode(Fig. 8). Fresh sample exhibited an even morphology consisting of decent spheres. Even though the majority of the particles preserved this morphology, some cracked and decomposed particles were observed for used particles.

To investigate the effect of partial O_2 pressure on the cyclic stability of CML, the fluidized bed tests were carried out under two different O_2 concentration(Fig. 9). When the partial O_2 pressure in the system was

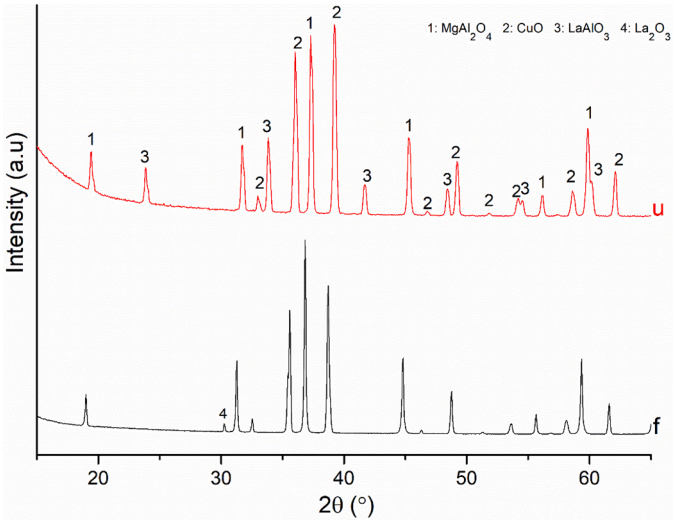

Fig. 7. XRD patterns of fresh and used $MgAl_2O_2$-La_2O_3 supported CuO sample.

0,05 atm, CML exhibited an outstanding performance compare to the case in which the partial O_2 pressure was 0,21 atm as air. This result was expected since equilibrium partial O_2 pressure of Cu-oxides is lower than 0,21 for the relevant temperature of this study [21,54]. However, 21 vol. % O_2 concentration was also used on the sample to reveal the result in case of using pure air (non-diluted with N_2) in the system.

4. Discussion

In this study, ZrO_2, La_2O_3, $MgAl_2O_4$ and CeO_2 supported Cu based oxide materials were tested as potential thermochemical energy storage materials. The chemical reactions and oxides systems used are similar in TCES and chemical looping oxygen uncoupling (CLOU). Therefore the

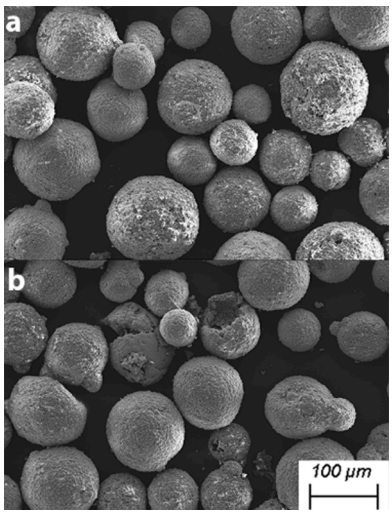

Fig. 8. Secondary electron SEM micrograph of fresh (a) and used (b) $MgAl_2O_2$-La_2O_3 supported CuO sample.

materials which have previously been used in CLOU applications [25,33,55–62] were tested as potential energy storage materials in this study. The purpose of the support materials are to increase the operational temperature, compared to pure Cu-oxides; and decrease the agglomeration tendency [26,32]. For this reason, it was important to avoid possible new compound forming between CuO and the support material, which may decrease the performance of the CuO/Cu_2O system. After the tests, there were no formation of phases observed which may deactivate the copper oxides. However, $La_2Zr_2O_7$, $LaAlO_3$ and $Ce_{0,75}La_{0,25}O_2$ was formed which could not be observed during initial synthesis of the materials. Even though newly formed compounds do not directly affect the copper oxide, thermal stability of the material is important. As outstanding thermal stability was reported for $La_2Zr_2O_7$ and $LaAlO_3$, formation of these compounds may affect the active materials lifetime in a positive manner. In addition to this, no defluidization was observed during the tests which means that agglomeration of the sample was avoided . Visual inspection after the fluidized bed tests also revealed neither sintering nor agglomeration in the bed.

Table 3 is given to summarize the results. Both thermal analysis and fluidized bed reactor tests were carried out in this work. Fluidized bed reactor tests enable to use comparably large amount of samples which may be a representative of more homogeneous sampling and also show the physical behaviour of the particles such as attrition or tendency for agglomeration. On the other hand, more accurate temperature and weight changes can be obtained by thermal analysis. For this reason, these two methods are considered as supplementary. Theoretical weight gain and weight loss for reduction of CuO to Cu_2O are 11,18wt.% and 10,06wt.%, respectively. $MgAl_2O_4$ and $MgAl_2O_4$-La_2O_3 supported CuO showed the best O_2 release/consumption capacity in both fluidized bed reactor test and thermal analysis among the tested samples, which are closer to the theoretical weight gain and loss values. In all fluidized bed test, the intermittent oxidation was observed most likely caused by the slow kinetics of reoxidation. For each sample, the oxygen uptake after the reduction got slower during the cooling and carried over with the following heating step. In fluidized bed reactor tests, the reduction peak temperatures were only 25-40°C higher than the obtained in the thermal analysis. However, the observed oxidation peak temperatures in thermal analysis were significantly higher than fluidized bed reactor tests for CZL, CML, and CCL. This difference most likely occurred due to the formation of new compounds.

The development of supported CuO oxides is necessary regarding to reversibility, reactivity loss over cycles and sintering in order to obtain cost effective, environmentally friendly and for large scale applications. The support materials used in this study showed very good performance regarding to the cyclic stability of the active phase. Even though, the high purity support materials are just slightly cheaper than the pure copper oxides, they may increase the lifetime of the active material. In

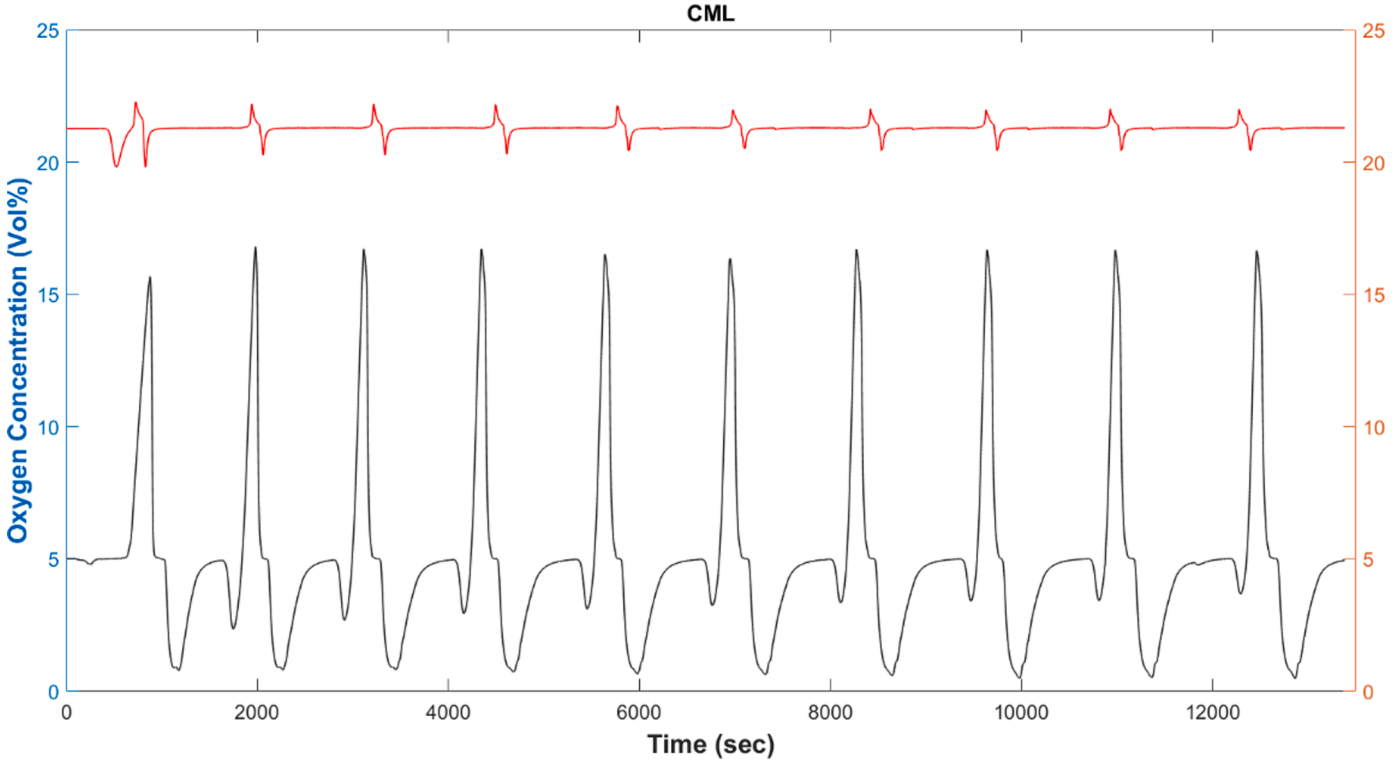

Fig. 9. Comparison of the cyclic stability of the $MgAl_2O_2$-La_2O_3 supported CuO sample under 5 vol.% O_2 and 21 vol.% O_2 atmosphere in the fluidized bed test.

Table 3
Summary of the results of the cyclic stability tests in the fluidized bed reactor and thermal analysis.

Sample	Fluidized Bed Reactor Tests				Thermal Analysis			
	Reduction Peak Temperature (T_{peak})	Peak Max. O_2/ Release (vol. %)	Oxidation Peak Temperature (T_{peak})	Peak Min. O_2/ Consumption (vol. %)	Reduction Peak Temperature (T_{peak})	Weight Loss (wt. %)	Oxidation Peak Temperature (T_{peak})	Weight Gain (wt. %)
CZ	1020	10,99	900	1,8	990	0,98	920	0,8
CZL	1025	12,11	890	1,46	980	1,30	950	1,03
CM	1010	16,51	870	0,53	985	1,01	910	1,06
CML	1010	16,71	820	0,54	970	3,07	920	2,4
CC	1020	11,20	840	1,76	990	0,5	890	0,5
CCL	1020	12,58	820	0,25	980	0,8	920	0,7

Table 4
Heat content of the relevant oxides [63].

Oxides	$H^{\circ}_{1200} - H^{\circ}_{298}\left(\frac{kJ}{mole}\right)$
CuO	47
Cu_2O	67
ZrO_2	64
La_2O_3	114
$MgAl_2O_4$	147
$LaAlO_3$	109

addition to this, as the redox reactions of copper oxides take place at high temperatures, the sensible heat form of the storage of interest is also important. In Table 4, the heat content of the supporting oxides used in this study is given. From this point of view, even the non-active, support phase of the sample contributes for storing the heat. Among the tested samples in the study, CM and CML are very promising in terms of both cost effectivity and abundancy of MgO and Al_2O_3. Especially, CML showed the best performance with the highest specific energy content (925 and 1050 kJ/kg CML for reduction and oxidation, respectively) which may lead the reduction of the raw material costs.

5. Conclusion

In the present study, ZrO_2, $MgAl_2O_4$, CeO_2 and La_2O_3 were used as support materials to improve the cyclic stability performance of copper oxide materials for thermochemical energy storage applications. Even though CuO has excellent properties for thermochemical energy storage applications, use of pure CuO is limited due to its high decomposition temperature in air (1034°C) and low agglomeration resistance above the relevant temperature limits. Among the oxides which have been reported in the literature as support material for CuO, ZrO_2, $MgAl_2O_4$, CeO_2 and La_2O_3 were chosen owing to their proved success in the previous studies for other applications. The cyclic stability tests were carried out in a fluidized bed reactor. Fluidized bed tests are significantly promoted for thermochemical energy storage application studies as it enables physical testing of large amount of samples. Obtained results were also compared to results from the thermal analysis. Among the tested samples, $MgAl_2O_4$ and $MgAl_2O_4/La_2O_3$ supported CuO exhibited the best O_2 release/consumption capacity. In fluidized bed tests, CML which showed the best performance exhibited 1,5 times more O_2 release and 3 times more O_2 consumption than CZ which showed the poorest performance. For STA, CML performed averagely 6 times more weight loss and 5 times more weight gain than the poorest performance CC. As $MgAl_2O_4$ is comparably cheaper than other used oxides and the amount of La_2O_3 was quite low (5 wt.%) in the composition, this result was quite promising for the application. The poorest O_2 release/consumption capacity was observed for CeO_2 supported CuO which was quite unexpected since CeO_2 has been used for its catalyst effect on Cu. However, CeO_2 and La_2O_3 supported CuO samples exhibited an identical cyclic behavior and reversibility which are important for material`s lifetime.

CRediT authorship contribution statement

Duygu Yilmaz: Writing - original draft, Investigation, Conceptualization. **Esraa Darwish:** Investigation, Methodology. **Henrik Leion:** Conceptualization, Writing - review & editing, Supervision.

Declaration of Competing Interest

The authors declare that they have no known competing financial interests or personal relationships that could have appeared to influence the work reported in this paper.

Acknowledgement

This work was funded by Åforsk (project number: 21285128).

Supplementary materials

Supplementary material associated with this article can be found, in the online version, at doi:10.1016/j.est.2020.102012.

References

[1] M. Kubicek, A.H. Bork, J.L.M. Rupp, Perovskite oxides – a review on a versatile material class for solar-to-fuel conversion processes, J, Mater. Chem. A. 5 (2017) 11983–12000, https://doi.org/10.1039/C7TA00987A.
[2] A. Evans, V. Strezov, T.J. Evans, Assessment of utility energy storage options for increased renewable energy penetration, Renew. Sustain. Energy Rev. 16 (2012) 4141–4147, https://doi.org/10.1016/j.rser.2012.03.048.
[3] P. Pardo, A. Deydier, Z. Anxionnaz-minvielle, S. Rougé, M. Cabassud, P. Cognet, P. Pardo, A. Deydier, Z. Anxionnaz-minvielle, S. Rougé, M. Cabassud, A review on high temperature thermochemical heat energy storage, Renew. Sustain. Energy Rev. 32 (2016) 591–610.
[4] L.F. Zalba, M.J B, H.M. Cabeza, Review on Phase changing materials to store energy, Appl. Therm. Eng. 23 (2003) 251–283, https://doi.org/10.1016/S1359-4311(02)00192-8.
[5] E. Guy, Solar heat storage using chemical reactions, J. Solid State Chem. 22 (1977) 51–61.
[6] W.E. Wentworth, E. Chen, Simple thermal decomposition reactions for storage of solar thermal energy, Solar Energy 18 (1976) 205–214, https://doi.org/10.1016/0038-092X(76)90019-0.
[7] L. André, S. Abanades, G. Flamant, Screening of thermochemical systems based on solid-gas reversible reactions for high temperature solar thermal energy storage, Renew. Sustain. Energy Rev. 64 (2016) 703–715, https://doi.org/10.1016/j.rser.2016.06.043.
[8] L. André, S. Abanades, L. Cassayre, Experimental investigation of Co-Cu, Mn-Co, and Mn-Cu redox materials applied to solar thermochemical energy storage, ACS Appl. Energy Mater. 1 (2018) 3385–3395, https://doi.org/10.1021/acsaem.8b00554.
[9] B. Michel, N. Mazet, S. Mauran, D. Stitou, J. Xu, Thermochemical process for seasonal storage of solar energy: characterization and modeling of a high density reactive bed, Energy 47 (2012) 553–563, https://doi.org/10.1016/j.energy.2012.09.029.
[10] P. Pardo, A. Deydier, Z. Anxionnaz-Minvielle, S. Rougé, M. Cabassud, P. Cognet, A review on high temperature thermochemical heat energy storage, Renew. Sustain. Energy Rev. 32 (2014) 591–610, https://doi.org/10.1016/j.rser.2013.12.014.
[11] S. Wu, C. Zhou, E. Doroodchi, R. Nellore, B. Moghtaderi, A review on high-temperature thermochemical energy storage based on metal oxides redox cycle, Energy Convers. Manage. 168 (2018) 421–453, https://doi.org/10.1016/j.enconman.2018.05.017.

[12] L. Duan, D. Godino, V. Manovic, F. Montagnaro, E.J. Anthony, Cyclic oxygen release characteristics of bifunctional copper oxide/calcium oxide composites, Energy Technol. 4 (2016) 1171–1178, https://doi.org/10.1002/ente.201600028.
[13] T. Block, M. Schmücker, Metal oxides for thermochemical energy storage: a comparison of several metal oxide systems, Solar Energy 126 (2016) 195–207, https://doi.org/10.1016/j.solener.2015.12.032.
[14] A.J. Carrillo, D.P. Serrano, P. Pizarro, J.M. Coronado, Manganese oxide-based thermochemical energy storage: modulating temperatures of redox cycles by Fe-Cu co-doping, J. Energy Storage 5 (2016) 169–176, https://doi.org/10.1016/j.est.2015.12.005.
[15] M. Silakhori, M. Jafarian, M. Arjomandi, G.J. Nathan, Thermogravimetric analysis of Cu, Mn, Co, and Pb oxides for thermochemical energy storage, J. Energy Storage 23 (2019) 138–147, https://doi.org/10.1016/j.est.2019.03.008.
[16] M. Deutsch, F. Horvath, C. Knoll, D. Lager, C. Gierl-Mayer, P. Weinberger, F. Winter, High-temperature energy storage: kinetic investigations of the CuO/Cu2O reaction cycle, Energy Fuels 31 (2017) 2324–2334, https://doi.org/10.1021/acs.energyfuels.6b02343.
[17] T. Mattisson, A. Lyngfelt, H. Leion, Chemical-looping with oxygen uncoupling for combustion of solid fuels, Int. J. Greenh. Gas Control 3 (2009) 11–19, https://doi.org/10.1016/j.egypro.2009.01.060.
[18] B. Wong, Thermochemical heat storage for concentrated solar power, thermochemical system reactor design for thermal energy storage, Ind. Eng. Chem. (2011), https://doi.org/10.2172/1039304.
[19] E. Alonso, C. Pérez-Rábago, J. Licurgo, E. Fuentealba, C.A. Estrada, First experimental studies of solar redox reactions of copper oxides for thermochemical energy storage, Solar Energy 115 (2015) 297–305, https://doi.org/10.1016/j.solener.2015.03.005.
[20] M. Hänchen, A. Stiel, Z.R. Jovanovic, A. Steinfeld, Thermally driven copper oxide redox cycle for the separation of oxygen from gases, Ind. Eng. Chem. Res. 51 (2012) 7013–7021, https://doi.org/10.1021/ie202474s.
[21] Q. Imtiaz, D. Hosseini, C.R. Müller, Review of oxygen carriers for chemical looping with oxygen uncoupling (CLOU): thermodynamics, material development, and synthesis, Energy Technol. 1 (2013) 633–647, https://doi.org/10.1002/ente.201300099.
[22] M. Rydén, D. Jing, M. Källén, H. Leion, A. Lyngfelt, T. Mattisson, CuO-based oxygen-carrier particles for chemical-looping with oxygen uncoupling - experiments in batch reactor and in continuous operation, Ind. Eng. Chem. Res. 53 (2014) 6255–6267, https://doi.org/10.1021/ie4039983.
[23] V. Frick, M. Rydén, H. Leion, Investigation of Cu–Fe and Mn–Ni oxides as oxygen carriers for chemical-looping combustion, Fuel Process. Technol. 150 (2016) 30–40, https://doi.org/10.1016/j.fuproc.2016.04.032.
[24] M. Keller, J. Fung, H. Leion, T. Mattisson, Cu-impregnated alumina/silica bed materials for chemical looping reforming of biomass gasification gas, Fuel 180 (2016) 448–456, https://doi.org/10.1016/j.fuel.2016.04.024.
[25] M. Arjmand, A. Azad, H. Leion, A. Lyngfelt, T. Mattisson, Prospects of Al 2 O 3 and MgAl 2 O 4 -supported CuO oxygen carriers in chemical-looping combustion (CLC) and chemical-looping with oxygen uncoupling (CLOU), Energy Fuels 25 (2011) 5493–5502, https://doi.org/10.1021/ef201329x.
[26] C.K. Clayton, K.J. Whitty, Measurement and modeling of decomposition kinetics for copper oxide-based chemical looping with oxygen uncoupling, Appl Energy 116 (2014) 416–423, https://doi.org/10.1016/j.apenergy.2013.10.032.
[27] M.S.C. Chan, H.G. Baldovi, J.S. Dennis, Enhancing the capacity of oxygen carriers for selective oxidations through phase cooperation: bismuth oxide and ceria-zirconia, Catal. Sci. Technol. 8 (2018) 887–897, https://doi.org/10.1039/c7cy01992k.
[28] L.F. de Diego, P. Gayán, F. García-Labiano, J. Celaya, A. Abad, J. Adánez, Impregnated CuO/Al2O3 oxygen carriers for chemical-looping combustion: avoiding fluidized bed agglomeration, Energy Fuels 19 (2005) 1850–1856, https://doi.org/10.1021/ef050052f.
[29] M. Arjmand, A.M. Azad, H. Leion, M. Rydén, T. Mattisson, ZrO2 supported CuO oxygen carriers for chemical-looping with oxygen uncoupling (CLOU), Energy Procedia 37 (2013) 550–559, https://doi.org/10.1016/j.egypro.2014.07.009.
[30] A. Hedayati, A.M. Azad, M. Rydén, H. Leion, T. Mattisson, Evaluation of novel ceria-supported metal oxides as oxygen carriers for chemical-looping combustion, Ind Eng Chem Res 51 (2012) 12796–12806, https://doi.org/10.1021/ie300168j.
[31] D. Jing, T. Mattisson, M. Ryden, P. Hallberg, A. Hedayati, J. Van Noyen, F. Snijkers, A. Lyngfelt, Innovative oxygen carrier materials for chemical-looping combustion, Energy Procedia 37 (2013) 645–653, https://doi.org/10.1016/j.egypro.2013.05.152.
[32] Y. Cao, H.Y. Zhao, S.P. Sit, W.P. Pan, Lanthanum-promoted copper-based oxygen carriers for chemical looping combustion process, J. Therm. Anal. Calorim. 116 (2014) 1257–1266, https://doi.org/10.1007/s10973-013-3628-8.
[33] T. Mattisson, H. Leion, A. Lyngfelt, Chemical-looping with oxygen uncoupling using CuO/ZrO2 with petroleum coke, Fuel 88 (2009) 683–690, https://doi.org/10.1016/j.fuel.2008.09.016.
[34] M. Keller, H. Leion, T. Mattisson, H. Thunman, Investigation of natural and synthetic bed materials for their utilization in chemical looping reforming for tar elimination in biomass-derived gasification gas, Energy Fuels 28 (2014) 3833–3840, https://doi.org/10.1021/ef500369c.
[35] M. Arjmand, M. Keller, H. Leion, T. Mattisson, A. Lyngfelt, Oxygen release and oxidation rates of MgAl2O4- supported CuO oxygen carrier for chemical-looping combustion with oxygen uncoupling (CLOU), Energy Fuels 26 (2012) 6528–6539, https://doi.org/10.1021/ef3010064.
[36] I. Adánez-Rubio, P. Gayán, A. Abad, F. García-Labiano, L.F.F. de Diego, J. Adánez, Kinetic analysis of a Cu-based oxygen carrier: relevance of temperature and oxygen partial pressure on reduction and oxidation reactions rates in chemical looping with oxygen uncoupling (CLOU), Chem. Eng. J. 256 (2014) 69–84, https://doi.org/10.1016/j.cej.2014.06.102.
[37] D. Jing, T. Mattisson, M. Ryden, P. Hallberg, A. Hedayati, J. Van Noyen, F. Snijkers, A. Lyngfelt, Innovative oxygen carrier materials for chemical-looping combustion, Energy Procedia 37 (2013) 645–653, https://doi.org/10.1016/j.egypro.2013.05.152.
[38] H. Leion, V. Frick, F. Hildor, Experimental method and setup for laboratory fluidized bed reactor testing, Energies (2018) 11, https://doi.org/10.3390/en11102505.
[39] E.I. Leonidova, I.A. Leonidov, M.V. Patrakeev, V.L. Kozhevnikov, Oxygen non-stoichiometry, high-temperature properties, and phase diagram of CaMnO 3-δ, J. Solid State Electrochem. 15 (2011) 1071–1075, https://doi.org/10.1007/s10008-010-1288-1.
[40] C. Tregambi, F. Montagnaro, P. Salatino, R. Solimene, Directly irradiated fluidized bed reactors for thermochemical processing and energy storage: application to calcium looping, in: AIP Conference Proceedings 1850, 2017, https://doi.org/10.1063/1.4984456.
[41] S. Ströhle, A. Haselbacher, Z.R. Jovanovic, A. Steinfeld, The effect of the gas-solid contacting pattern in a high-temperature thermochemical energy storage on the performance of a concentrated solar power plant, Energy Environ. Sci. 9 (2016) 1375–1389, https://doi.org/10.1039/c5ee03204k.
[42] T. Block, N. Knoblauch, M. Schmücker, The cobalt-oxide/iron-oxide binary system for use as high temperature thermochemical energy storage material, Thermochimica Acta 577 (2014) 25–32, https://doi.org/10.1016/j.tca.2013.11.025.
[43] C. Agrafiotis, M. Roeb, M. Schmücker, C. Sattler, Exploitation of thermochemical cycles based on solid oxide redox systems for thermochemical storage of solar heat. Part 1: testing of cobalt oxide-based powders, Solar Energy 102 (2014) 189–211, https://doi.org/10.1016/j.solener.2013.12.032.
[44] S. Tescari, C. Agrafiotis, S. Breuer, L. De Oliveira, M. Neises-Von Puttkamer, M. Roeb, C. Sattler, Thermochemical solar energy storage via redox oxides: materials and reactor/heat exchanger concepts, Energy Procedia 49 (2013) 1034–1043, https://doi.org/10.1016/j.egypro.2014.03.111.
[45] G. Karagiannakis, C. Pagkoura, A. Zygogianni, S. Lorentzou, A.G. Konstandopoulos, Monolithic ceramic redox materials for thermochemical heat storage applications in CSP plants, Energy Procedia 49 (2014) 820–829, https://doi.org/10.1016/j.egypro.2014.03.089.
[46] M. Neises, S. Tescari, L. de Oliveira, M. Roeb, C. Sattler, B. Wong, Solar-heated rotary kiln for thermochemical energy storage, Solar Energy 86 (2012) 3040–3048, https://doi.org/10.1016/j.solener.2012.07.012.
[47] S.M. Babiniec, E.N. Coker, A. Ambrosini, J.E. Miller, ABO3 (A = La, Ba, Sr, K; B = Co, Mn, Fe) perovskites for thermochemical energy storage, in: AIP Conference Proceedings 1734, 2016, https://doi.org/10.1063/1.4949104.
[48] K.T. Jacob, C.B. Alcock, Thermodynamics of CuAlO2 and CuAl2O4 and phase equilibria in the system Cu2O-Cu0-Al2O3, J. Am. Ceram. Soc. 58 (1974) 192–195.
[49] C.K. Clayton, H.Y. Sohn, K.J. Whitty, Oxidation kinetics of Cu2O in oxygen carriers for chemical looping with oxygen uncoupling, Ind. Eng. Chem. Res. 53 (2014) 2976–2986, https://doi.org/10.1021/ie402495a.
[50] S.S. Jahromy, F. Birkelbach, C. Jordan, C. Huber, M. Harasek, A. Werner, F. Winter, Impact of partial pressure, conversion, and temperature on the oxidation reaction kinetics of Cu 2 O to CuO in thermochemical energy storage, Energies (2019) 12, https://doi.org/10.3390/en12030508.
[51] C. Prieto, P. Cooper, A.I. Fernández, L.F. Cabeza, Review of technology: thermochemical energy storage for concentrated solar power plants, Renew. Sustain. Energy Rev. 60 (2016) 909–929, https://doi.org/10.1016/j.rser.2015.12.364.
[52] A.H. McDaniel, E.C. Miller, D. Arifin, A. Ambrosini, E.N. Coker, R. O'Hayre, W. C. Chueh, J. Tong, Sr- and Mn-doped LaAlO3-δ for solar thermochemical H 2 and CO production, Energy Environ. Sci. 6 (2013) 2424–2428, https://doi.org/10.1039/c3ee41372a.
[53] S.V. Ushakov, A. Navrotsky, Direct measurement of fusion enthalpy of LaAlO 3 and comparison of energetics of melt, glass, and amorphous thin films, J. Am. Ceram. Soc. 97 (2014) 1589–1594, https://doi.org/10.1111/jace.12785.
[54] I. Barin, O. Knacke, Thermochemical Properties of Inorganic Substances, Springer, Berlin Heidelberg, 1973.
[55] P. Gayán, C.R. Forero, A. Abad, L.F. De Diego, F. García-Labiano, J. Adánez, Effect of support on the behavior of Cu-based oxygen carriers during long-term CLC operation at temperatures above 1073 K, Energy Fuels 25 (2011) 1316–1326, https://doi.org/10.1021/ef101583w.
[56] C.R. Forero, P. Gayán, F. García-Labiano, L.F. de Diego, A. Abad, J. Adánez, High temperature behaviour of a CuO/γAl2O3 oxygen carrier for chemical-looping combustion, Inte. J. Greenh. Gas Control 5 (2011) 659–667, https://doi.org/10.1016/j.ijggc.2011.03.005.
[57] M. Arjmand, A.-M. Azad, H. Leion, T. Mattisson, A. Lyngfelt, Evaluation of CuAl2O4 as an oxygen carrier in chemical-looping combustion, Ind. Eng. Chem. Res. (2012) 51, https://doi.org/10.1021/ie300427w.
[58] J. Adanez, A. Abad, F. Garcia-Labiano, P. Gayan, L.F. De Diego, Progress in chemical-looping combustion and reforming technologies, Prog. Energy Comb. Sci. 38 (2012) 215–282, https://doi.org/10.1016/j.pecs.2011.09.001.
[59] P. Gayán, I. Adánez-Rubio, A. Abad, L.F. De Diego, F. García-Labiano, J. Adánez, Development of Cu-based oxygen carriers for chemical-looping with oxygen uncoupling (CLOU) process, Fuel 96 (2012) 226–238, https://doi.org/10.1016/j.fuel.2012.01.021.
[60] P. Moldenhauer, M. Rydén, T. Mattisson, A. Lyngfelt, Chemical-looping combustion and chemical-looping with oxygen uncoupling of kerosene with Mn-

and Cu-based oxygen carriers in a circulating fluidized-bed 300 W laboratory reactor, Fuel Process. Technol. 104 (2012) 378–389, https://doi.org/10.1016/j.fuproc.2012.06.013.

[61] I. Adánez-Rubio, P. Gayán, A. Abad, L.F. De Diego, F. García-Labiano, J. Adánez, Evaluation of a spray-dried CuO/MgAl 2O 4 oxygen carrier for the chemical looping with oxygen uncoupling process, Energy Fuels 26 (2012) 3069–3081, https://doi.org/10.1021/ef3002229.

[62] A. Abad, I. Adánez-Rubio, P. Gayán, F. García-Labiano, L.F. de Diego, J. Adánez, Demonstration of chemical-looping with oxygen uncoupling (CLOU) process in a 1.5kWthcontinuously operating unit using a Cu-based oxygen-carrier, Int. J. Greenh. Gas Control 6 (2012) 189–200, https://doi.org/10.1016/j.ijggc.2011.10.016.

[63] C.W. Bale, E. Bélisle, Fact-web suite of interactive programs, (n.d.). www.factsage.com.